Available online at www.sciencedirect.com
ScienceDirect
Materials Research Bulletin 43 (2008) 2130–2136
Materials Research Bulletin
www.elsevier.com/locate/matresbu

Polyol-mediated syntheses and characterizations of $NaYF_4$, $NH_4Y_3F_{10}$ and YF_3 nanocrystals/sub-microcrystals

Ruifei Qin [a,b], Hongwei Song [a,*], Guohui Pan [a,b], Lanying Hu [a,b], Hongquan Yu [a,b], Suwen Li [a,b], Xue Bai [a,b], Libo Fan [a,b], Qilin Dai [a,b], Xinguang Ren [a], Haifeng Zhao [a], Tie Wang [a]

[a] *Key Laboratory of Excited State Physics, Changchun Institute of Optics, Fine Mechanics and Physics, Chinese Academy of Sciences, 16 Eastern Nan-Hu Road, Changchun 130033, PR China*
[b] *Graduate School of Chinese Academy of Sciences, Beijing 100039, PR China*

Received 20 March 2007; received in revised form 18 July 2007; accepted 15 September 2007
Available online 29 September 2007

Abstract

In this paper, $NaYF_4$ nanocrystals and $NH_4Y_3F_{10}$ sub-microcrystals were prepared using a polyol method. After being annealed, $NH_4Y_3F_{10}$ can convert into YF_3, which is a very efficient host matrix for upconversion. The structures of obtained $NaYF_4$, $NH_4Y_3F_{10}$ and YF_3 samples are pure cubic phase, a mixture of cubic and hexagonal phase and pure orthorhombic phase, respectively. The size of obtained $NaYF_4$ nanocrystals is about 20 nm, and those of $NH_4Y_3F_{10}$ and YF_3 sub-microcrystals are both about 200 nm. When co-doped with Er^{3+} and Yb^{3+}, $NaYF_4$ and YF_3 samples can emit bright light under 978 nm excitation. Upconversion mechanisms in Yb^{3+}/Er^{3+} co-doped $NaYF_4$ and YF_3 samples were discussed.

Keywords: A. Fluorides; B. Nanostructures; C. Luminescence

1. Introduction

As a very efficient host matrix for green and blue upconversion, sodium yttrium tetrafluoride ($NaYF_4$) in the nanometer size range has attracted considerable interest recently due to its potential use as biolabels [1–11]. Upconversion is the generation of higher energy light from lower energy radiation. At ambient temperature and pressure, the $NaYF_4$ exists in two polymorphs: the hexagonal ($Na_{1.5}Y_{1.5}F_6$ type) structure and the cubic (fluorite type) one [12]. In the past few years, many papers reported the synthesis of nanoscale $NaYF_4$. $NaYF_4$:Yb, Er nanocrystals were synthesized using a co-precipitation method and demonstrated to be promising upconversion biolabels [3]. Cubic $NaYF_4$ nanoparticles were prepared hydrothermally in the presence of surfactants or chelators [12,13]. Li's group synthesized hexagonal $NaYF_4$:Yb, Er nanoparticles using a solvothermal route, and combining magnetic separation and concentration technology and fluorescence resonant energy transfer technology they applied these nanoparticles to the sensitive detection of trace amounts of targeted biomolecules [4–6]. Very recently, high-quality cubic and hexagonal $NaYF_4$ nanocrystals were synthesized via the co-thermolysis of Na (CF_3COO) and Y ($CF_3COO)_3$ precursors [7–11].

* Corresponding author. Fax: +86 431 86176320.
E-mail address: hwsong2005@yahoo.com.cn (H. Song).

0025-5408/$ – see front matter © 2007 Elsevier Ltd. All rights reserved.
doi:10.1016/j.materresbull.2007.09.019

MLn_3F_{10} (M = alkaline metal, NH_4^+ and Ln = rare earth) is a big family of compounds including many useful materials, such as KY_3F_{10}, which has great potential as a host of the solid-state laser. Regarding the ionic radii and crystal structures of the MLn_3F_{10} family, ammonium compounds are particularly interesting, because the ionic radius (Pauling) of ammonium (1.48 Å) is comparable with those of K^+ (1.33 Å) and Rb^+ (1.48 Å) [14]. $NH_4Ln_3F_{10}$ (Ln = Dy, Ho, Y, Er, Tm) has been synthesized using a hydrothermal method [14]. Cubic $NH_4Ho_3F_{10}$, $NH_4Er_3F_{10}$ and $NH_4Tm_3F_{10}$ could be obtained by precipitation from a solution containing ammonium ions [15].

The polyol method is well-suited for the preparation of nanoparticles, in which a high-boiling alcohol (e.g. diethylene glycol, DEG, bp 246 °C) serves as both a solvent and a stabilizer that limits particle growth and prohibits agglomeration [16,17]. Many kinds of materials, such as metal [18], oxides [19–21], phosphates [22,23], and binary fluorides [24–26] in the nanometer size range have been synthesized through this method. In this paper, we synthesized $NaYF_4$ nanocrystals and $NH_4Y_3F_{10}$ sub-microcrystals using this method. After being annealed, $NH_4Y_3F_{10}$ can convert into YF_3, which is a very efficient host matrix for upconversion.

2. Experimental

2.1. Syntheses

All chemicals were of analytical grade and used as received without further purification. Deionized water was used throughout. In a typical synthesis of $NaYF_4$ nanocrystals, 0.672 g (0.016 mol) NaF was added to the mixture of 6 mL H_2O and 80 mL DEG. Afterwards a solution of 1.532 g (0.004 mol) $Y(NO_3)_3{\cdot}6H_2O$ in 20 mL DEG was added under vigorous stirring. After stirring for 12 h, it became transparent. The suspension was then transferred to a 250 mL round-bottomed flask and heated at 180 °C in a silicon oil bath under vigorous stirring and reflux for 2 h. After cooling to room temperature, the product was washed with absolute ethanol and water four times to remove DEG and reactants possibly remaining and was dried at 80 °C for 12 h in vacuum. It was referred to sample A.

The synthetic procedure of $NH_4Y_3F_{10}$ sub-microcrystals was similar to that of $NaYF_4$ nanocrystals, just using NH_4F instead of NaF. The molar ratio of reactants was NH_4F:$Y(NO_3)_3{\cdot}6H_2O$ = 10:3. The product was referred to sample B. After being annealed at 500 °C for 2 h, the yielded product was referred to sample C.

2.2. Methods

Crystal structure, morphology and size were obtained by powder X-ray diffraction (XRD, Rigaku D/max-rA diffractometer with CuKα radiation resource, λ = 1.54078 Å), field emission scanning electron microscopy (FE-SEM, Hitachi S-4800). The FTIR spectra were recorded on a Bio-Rad FTS-3000 (EXCALIBUR SERIES) spectrometer. Upconversion fluorescent spectra were recorded on a Hitachi F-4500 fluorescence spectrophotometer using a continuous 978 nm diode laser as the excitation source.

3. Results and discussion

3.1. Crystal structures and morphologies

The XRD patterns of the as-obtained products are depicted in Fig. 1. The diffraction peaks in curve 1a for sample A can be indexed to the pure cubic $NaYF_4$, which is in good agreement with that in literature (JCPDS card No. 77-2042). Estimated according to the widths of the diffraction peaks by Scherrer equation, the average crystallite size of sample A is 23 nm. We also synthesized $NaGdF_4$ nanocrystals using the polyol method. Although the same synthetic procedure is used, the as-obtained $NaYF_4$ and $NaGdF_4$ nanocrystals are cubic and hexagonal in structure, respectively. This difference may be ascribed to kinetic factors resulting from the slightly larger size of Gd^{3+} (1.107 Å) compared to Y^{3+} (1.075 Å) [27]. The diffraction peaks in curve 1b for sample B indicate that the product is a mixture of the cubic and the hexagonal (marked with asterisks) $NH_4Y_3F_{10}$, which is consistent with that in literature [14]. Generally, $NH_4Y_3F_{10}$ cannot be obtained by conventional solid-state reaction due to decomposition at high temperature. Our above results show that $NH_4Y_3F_{10}$ can be synthesized via the simple polyol method. After being annealed at 500 °C for 2 h, $NH_4Y_3F_{10}$ can convert into pure orthorhombic YF_3 (sample C), as is confirmed by the XRD pattern (JCPDS card

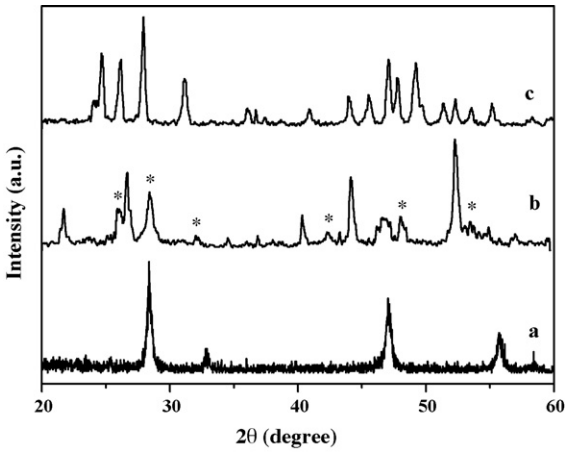

Fig. 1. XRD patterns of samples A (a), B (b) and C (c).

No. 74-0911). According to the widths of the diffraction peaks, samples B and C nearly have the same crystallite size with sample A based on the estimation by Scherrer equation.

Fig. 2 shows typical FE-SEM images of all samples. $NaYF_4$ nanocrystals (see Fig. 2a) aggregate to some degree and is ~20 nm in size, which is in good agreement with the result obtained from the XRD. As seen in Fig. 2b, $NH_4Y_3F_{10}$ sub-microcrystals are characterized by rough spheres and are about 200 nm in size. The size is much larger than that of $NaYF_4$ nanocrystals. According to the result obtained from XRD analysis, it is suggested that these $NH_4Y_3F_{10}$ sub-microcrystals should be composed of smaller crystallites. A higher magnification image of sample B (Fig. 2c) appears that $NH_4Y_3F_{10}$ sub-microcrystals are the assembly of nanocrystals. YF_3 sub-microcrystals obtained by annealing $NH_4Y_3F_{10}$ sub-microcrystals have the similar shape and nearly same size with $NH_4Y_3F_{10}$ sub-microcrystals (see Fig. 2d).

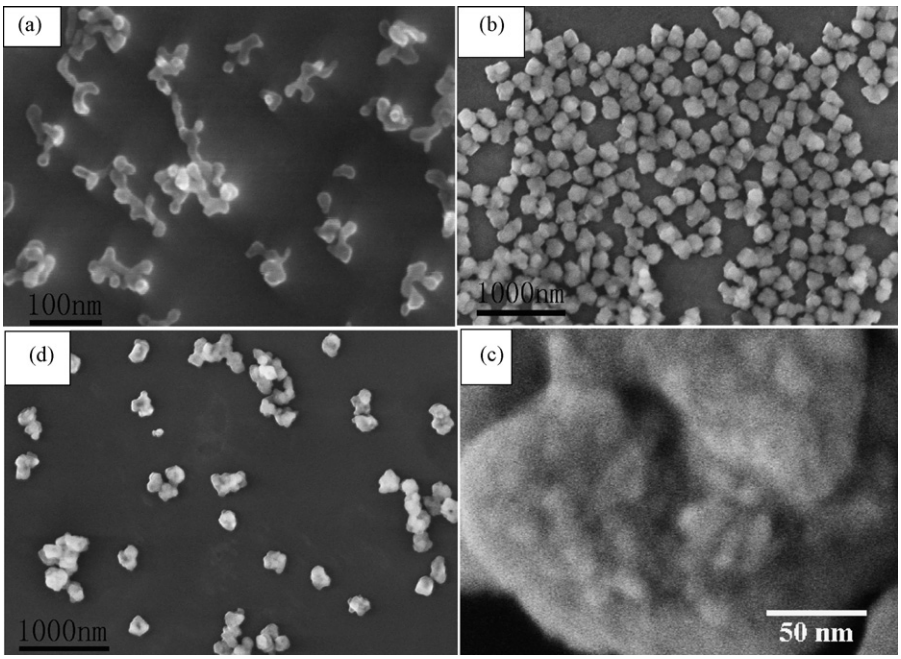

Fig. 2. FE-SEM images of samples A (a), B (b), B (c) and C (d).

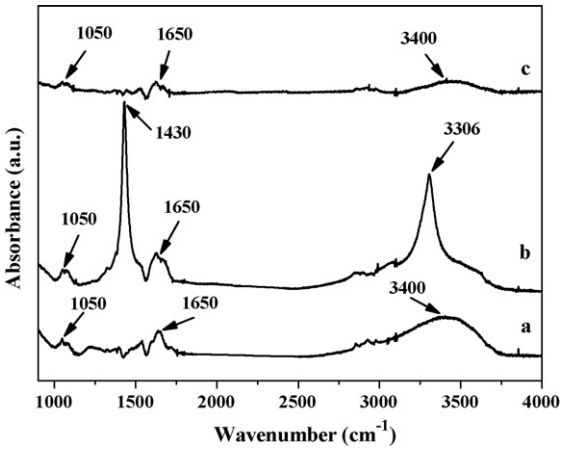

Fig. 3. FTIR spectra of samples A (a), B (b) and C (c).

3.2. FTIR spectra

Fig. 3 shows the FTIR spectra of all samples. In Fig. 3a, the bands around 3400 and 1650 cm^{-1}, respectively, originate from the stretching and bending vibrations of the OH^-groups of adsorbed H_2O. The peak at 1050 cm^{-1} is attributed to the C-OH stretching vibration mode, indicating the adsorption of a small amount of DEG on the surface of $NaYF_4$ nanocrystals. In Fig. 3b, besides absorption bands arising from the OH^- and C-OH vibrations, there exist absorption bands corresponding to the vibrations of the ammonium group. The bands at 1430 and 3306 cm^{-1} can be assigned to the bending and stretching vibrations of the ammonium group, respectively. In Fig. 3c, the bands arising from the ammonium group disappear due to the conversion of $NH_4Y_3F_{10}$ to YF_3 and those arising from the OH^- and C-OH vibrations still exist. Therefore after these samples are annealed at 500 °C for 2 h, some H_2O and DEG are still adsorbed on the surface of them.

3.3. Upconversion luminescence properties

To examine the feasibility of the as-obtained nanocrystals/sub-microcrystals as efficient upconversion host materials, the most frequently used upconversion ion Er^{3+} and the sensitizer ion Yb^{3+} were co-doped into samples A–C. Doped samples were prepared using the same synthetic procedure, except for adding 6% $Yb(NO_3)_3{\cdot}6H_2O$ and 1% $Er(NO_3)_3{\cdot}6H_2O$ into $Y(NO_3)_3{\cdot}6H_2O$. The upconversion emission of doped $NH_4Y_3F_{10}$ sample is invisible to the naked eye due to the quenching effect of ammonium with high-energy vibrations. Doped $NaYF_4$ and YF_3 samples both emit bright light under 978 nm excitation. Figs. 4 and 5 show upconversion emission spectra of doped $NaYF_4$ and YF_3 samples in the range of 500–700 nm, respectively, under 978 nm excitation. Green luminescence corresponding to the $^2H_{11/2}/^4S_{3/2} - {}^4I_{15/2}$ transitions locates in the wavelength region of 500–575 nm, and the $^4F_{9/2}$–$^4I_{15/2}$ transition-derived red luminescence ranges from 625 to 700 nm. Figs. 4 and 5, respectively, agree with what have been reported for Er^{3+} upconversion in cubic $NaYF_4$ nanocrystals and orthorhombic YF_3 sub-microcrystals prepared using other methods [1,8,9,28].

In the upconversion processes, the visible output intensity is in proportion to the nth power of the NIR excitation intensity, i.e., $I_{up} \propto (I_{exc})^n$, where I_{up} and I_{exc} represent the upconversion luminescence intensity and the NIR excitation intensity, respectively, and n is the number of photons required to produce an upconversion photon [29]. To understand how the $^2H_{11/2}/^4S_{3/2}$ and $^4F_{9/2}$ excited states are populated under 978 nm excitation, power dependence of upconversion luminescence intensity is plotted on a double logarithmic scale, as shown in the insets of Figs. 4 and 5. For doped $NaYF_4$ sample, the slopes are 1.7 and 2.0 for the red and green emissions, respectively, and for doped YF_3 sample, the slopes are 2.0 and 1.9 for the red and green emissions, respectively. These results indicate that two IR photons are required to produce a visible photon in doped $NaYF_4$ and YF_3 samples. Fig. 6 illustrates the energy level diagram and the possible mechanisms by which the $^2H_{11/2}/^4S_{3/2}$ and $^4F_{9/2}$ excited states are populated. Following 978 nm irradiation, the Yb^{3+} ion is excited from the ground state $^2F_{7/2}$ to the excited state $^2F_{5/2}$. Then the excited Yb^{3+}

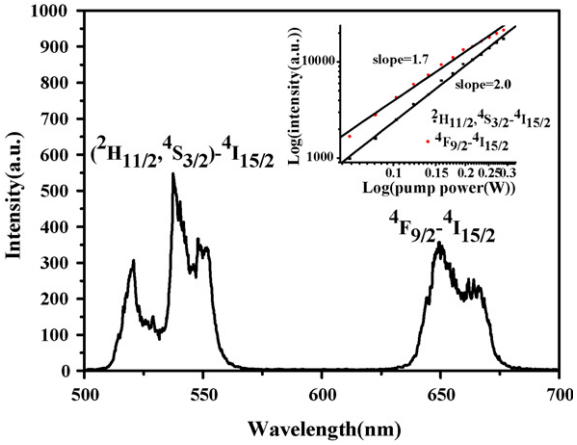

Fig. 4. Upconversion emission spectrum of sample A co-doped with 1% Er^{3+} and 6% Yb^{3+} under 978 nm excitation. The inset shows the upconversion luminescence intensity as a function of the laser power.

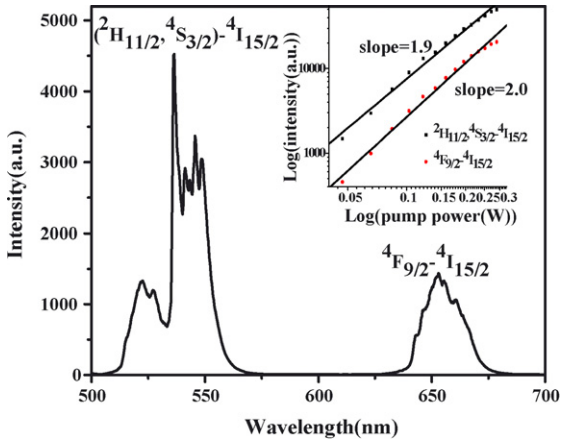

Fig. 5. Upconversion emission spectrum of sample C co-doped with 1% Er^{3+} and 6% Yb^{3+} under 978 nm excitation. The inset shows the upconversion luminescence intensity as a function of the laser power.

returns to the ground state and transfers its energy to Er^{3+} in the ground state $^4I_{15/2}$ and promotes it up to the $^4I_{11/2}$ intermediate excited state. Following this process, immediate energy transfer from another excited Yb^{3+} ion to Er^{3+} ion results in population of the $^4F_{7/2}$ state. Subsequent nonradiative relaxations of $^4F_{7/2}$–$^4S_{3/2}$/$^2H_{11/2}$ and $^4S_{3/2}$–$^4F_{9/2}$ populate the $^4S_{3/2}$/$^2H_{11/2}$ as well as the $^4F_{9/2}$ states. Er^{3+} in the $^4I_{11/2}$ state can also relax to the $^4I_{13/2}$ state by phonon emission and can subsequently be excited to the $^4F_{9/2}$ state through energy transfer, which is another possible path to populate the $^4F_{9/2}$ state and is more possible in nanocrystals [30–32].

The GRR value is defined as the intensity ratio between the green to red emission. From Figs. 4 and 5, it is obvious that the GRR value of $NaYF_4$ nanocrystals is smaller than that of YF_3 sub-microcrystals. It is known that the GRR value depends on preparation method, particle size, host matrix, crystallographic phase, doping level, excitation density, and so on [33–35]. For example, following excitation with 978 nm, the GRR value of nanocrystalline Y_2O_3:Er^{3+}, Yb^{3+} is much smaller than that of bulk Y_2O_3:Er^{3+}, Yb^{3+} [31,32]. The smaller particles often involve more surface defects, such as surface adsorption of H_2O and CO_2, which can effectively bridge the nonradiative transition channels of $^4I_{11/2}$–$^4I_{13/2}$ as well as $^4S_{3/2}$–$^4F_{9/2}$, leading to the decrease of GRR value. Generally, particles with lower upconversion efficiency show a lower GRR value [33]. For bulk materials, upconversion emission of cubic $NaYF_4$ is about half of that of YF_3 [34,36]. Compared with YF_3 sub-microcrystals, the smaller GRR value of $NaYF_4$ nanocrystals can mainly be attributed to the much smaller size and the lower upconversion efficiency of cubic $NaYF_4$ host matrix.

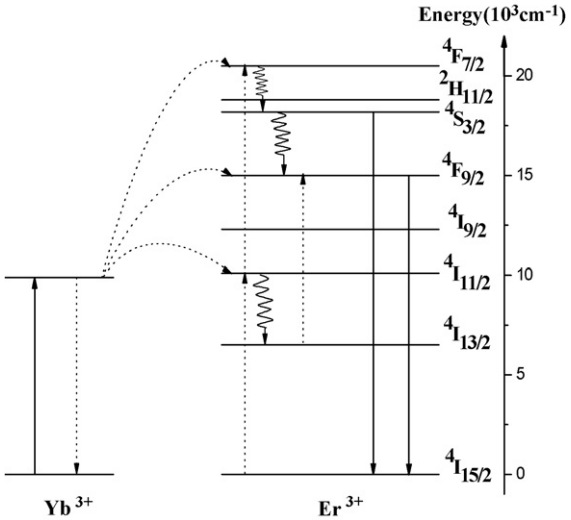

Fig. 6. The energy level diagrams for Yb^{3+}/Er^{3+} systems and upconversion luminescence processes under 978 nm excitation. The full, dotted, and curly arrows represent emission, energy transfer and multiphonon relaxation processes, respectively.

4. Conclusions

We synthesized $NaYF_4$, $NH_4Y_3F_{10}$ and YF_3 nanocrystals/sub-microcrystals via the polyol method and characterized them by XRD patterns, FE-SEM images, FTIR spectra. Yb^{3+}/Er^{3+} co-doped $NaYF_4$ nanocrystals and YF_3 sub-microcrystals emit bright red and green light under 978 nm excitation and have potential to be used in the field of bioassays. This method should be desirable to other ternary lanthanide fluoride compounds in the nanometer/sub-micrometer size range.

Acknowledgements

This work is supported by the National Nature Science Foundation of China (Grants 10374086 and 10504030) and Talent Youth Foundation of JiLin Province (Grants 20040105).

References

[1] S. Heer, K. Kompe, H.U. Gudel, M. Haase, Adv. Mater. 16 (23–24) (2004) 2102.
[2] H.C. Lu, G.S. Yi, S.Y. Zhao, D.P. Chen, L.H. Guo, J. Cheng, J. Mater. Chem. 14 (2004) 1336.
[3] G.S. Yi, H.C. Lu, S.Y. Zhao, Y. Ge, W.J. Yang, D.P. Chen, L.H. Guo, Nano. Lett. 4 (11) (2004) 2191.
[4] J.H. Zeng, J. Su, Z.H. Li, R.X. Yan, Y.D. Li, Adv. Mater. 17 (2005) 2119.
[5] L.Y. Wang, Y.D. Li, Chem. Commun. (24) (2006) 2557.
[6] L.Y. Wang, R.X. Yan, Z.Y. Hao, L. Wang, J.H. Zeng, H. Bao, X. Wang, Q. Peng, Y.D. Li, Angew. Chem. Int. Ed. 44 (37) (2005) 6054.
[7] H.X. Mai, Y.W. Zhang, R. Si, Z.G. Yan, L.D. Sun, L.P. You, C.H. Yan, J. Am. Chem. Soc. 128 (2006) 6426.
[8] J.C. Boyer, F. Vetrone, L.A. Cuccia, J.A. Capobianco, J. Am. Chem. Soc. 128 (23) (2006) 7444.
[9] J.C. Boyer, L.A. Cuccia, J.A. Capobianco, Nano. Lett. 7 (3) (2007) 847.
[10] G.S. Yi, G.M. Chow, Adv. Funct. Mater. 16 (2006) 2324.
[11] G.S. Yi, G.M. Chow, Chem. Mater. 19 (2007) 341.
[12] Z.J. Wang, F. Tao, L.Z. Yao, W.L. Cai, X.G. Li, J. Cryst. Growth 290 (2006) 296.
[13] X. Wang, J. Zhuang, Q. Peng, Y.D. Li, Inorg. Chem. 45 (17) (2006) 6661.
[14] Z.J. Kang, Y.X. Wang, F.T. You, J.H. Lin, J. Solid State Chem. 158 (2001) 358.
[15] A. Zalkin, D.H. Templeton, J. Am. Chem. Soc. 75 (1953) 2453.
[16] C. Feldmann, Adv. Funct. Mater. 13 (2) (2003) 101.
[17] C. Feldmann, Solid State Sci. 7 (2005) 868.
[18] J.Y. Chen, T. Herricks, Y.N. Xia, Angew. Chem. Int. Ed. 44 (2005) 2589.
[19] C. Feldmann, H.O. Jungk, Angew. Chem. Int. Ed. 40 (2001) 359.

[20] R. Bazzi, M.A. Flores, C. Louis, K. Lebbou, C. Dujardin, A. Brenier, W. Zhang, O. Tillement, E. Bernstein, P. Perriat, J. Lumin. 102–103 (2003) 445.
[21] R. Bazzi, M.A. Flores, C. Louis, K. Lebbou, W. Zhang, C. Dujardin, S. Roux, B. Mercier, G. Ledoux, E. Bernstein, P. Perriat, O. Tillement, J. Colloid Interf. Sci. 273 (2004) 191.
[22] C. Feldmann, H.O. Jungk, J. Mater. Sci. 37 (2002) 3251.
[23] Z.L. Wang, Z.W. Quan, J. Lin, J.Y. Fang, J. Nanosci. Nanotechnol. 5 (9) (2005) 1532.
[24] S. Eiden-Assmann, G. Maret, Mater. Res. Bull. 39 (2004) 21.
[25] Z.L. Wang, Z.W. Quan, P.Y. Jia, C.K. Lin, Y. Luo, Y. Chen, J. Fang, W. Zhou, C.J. O'Connor, J. Lin, Chem. Mater. 18 (2006) 2030.
[26] Y. Wei, F.Q. Lu, X.R. Zhang, D.P. Chen, Mater. Lett. 61 (2007) 1337.
[27] A. Aebischer, S. Heer, D. Biner, K. Kramer, M. Haase, H.U. Gudel, Chem. Phys. Lett. 407 (2005) 124.
[28] X. Liang, X. Wang, L.Y. Wang, R.X. Yan, Q. Peng, Y.D. Li, Eur. J. Inorg. Chem. (2006) 2186–2191.
[29] J.F. Suyver, A. Aebischer, S. García-Revilla, P. Gerner, H.U. Güdel, Phys. Rev. B 71 (2005) 125123.
[30] Y.Q. Lei, H.W. Song, L.M. Yang, L.X. Yu, Z.X. Liu, G.H. Pan, X. Bai, L.B. Fan, J. Chem. Phys. 123 (2005) 174710.
[31] F. Vetrone, J.C. Boyer, J.A. Capobianco, A. Speghini, M. Bettinelli, J. Phys. Chem. B 107 (2003) 1107.
[32] F. Vetrone, J.C. Boyer, J.A. Capobianco, A. Speghini, M. Bettinelli, J. Appl. Phys. 96 (2004) 661.
[33] H. Schafer, P. Ptacek, K. Kompe, M. Haase, Chem. Mater. 19 (2007) 1396.
[34] K.W. Kramer, D. Biner, G. Frei, H.U. Gudel, M.P. Hehlen, S.R. Luthi, Chem. Mater. 16 (2004) 1244.
[35] Z.H. Li, L.Z. Zheng, L.N. Zhang, L.Y. Xiong, J. Lumin. 126 (2007) 481.
[36] N. Menyuk, K. Dwight, J.W. Pierce, Appl. Phys. Lett. 21 (1972) 159.